Res Chem Intermed (2017) 43:2159–2174
DOI 10.1007/s11164-016-2752-z

An eco-friendly and magnetized biopolymer cellulose-based heterogeneous acid catalyst for facile synthesis of functionalized pyrimido[4,5-b]quinolines and indeno fused pyrido[2,3-d]pyrimidines in water

Fatemeh Osanlou[1] · Firouzeh Nemati[1] · Samaneh Sabaqian[1]

Received: 18 July 2016 / Accepted: 30 September 2016 / Published online: 11 October 2016

Abstract A cellulose-based magnetic nano-composite supported SO_3H group was synthesized and characterized using Fourier transform infrared spectroscopy, energy-dispersive X-ray spectroscopy, thermogravimetric analysis, X-ray diffraction, and scanning electron microscopy. Thereafter, its capability to promote the one-pot, three-component synthesis of pyrimido [4,5-b] quinolone and pyrido [2,3-d] pyrimidine derivatives was evaluated. The obtained results are indicative of excellent yields and short reaction times. The biopolymer based catalyst is readily recovered and reused several times without a decrease in yield.

✉ Firouzeh Nemati
fnemati_1350@yahoo.com; fnemati@semnan.ac.ir

[1] Department of Chemistry, Semnan University, Semnan, Iran

Graphical Abstract

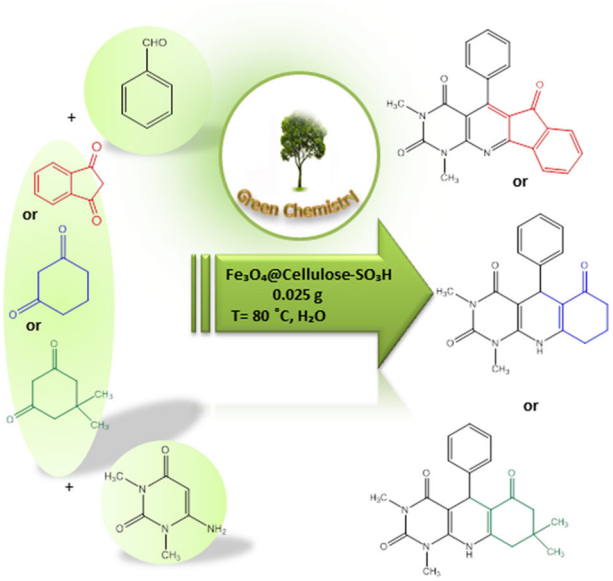

Keywords Magnetic cellulose · Nanocatalyst · Sulfonic acid · Green solvent

Introduction

Multi-component reactions are known as versatile synthesis tools for the assembly of novel and structurally complex molecules from simple starting materials in a minimum of reaction steps [1]. These reactions have emerged as a valuable method for the formation and breakage of carbon–carbon and carbon-heteroatom bonds in a one-pot and simple work-up procedure. The synthesis of highly functionalized quinolines illustrates the proper application of multi-component reactions because the quinoline moiety possesses promising biological activities, such as antimalarial, anticancer, antimicrobial [2], antiallergy, and anti-inflammatory activities, which essentially associate to the nature and the place of the substituents [3]. In addition to the abovementioned activities, pyridopyrimidins show a broad spectrum of biological and pharmacological activity, including antifloate, tyrosine kinase inhibitors, anti-aggressive [4], antitumor, cardiotonic, heptoprotactive, antifungal, antibronchitic [5], and calcium antagonist [6].

Recently, effort has been made in order to replace the traditional liquid inorganic homogeneous acid, with heterogeneous ones, because of their environmental, economical and industrial aspects. To address the aforementioned issues, the covalently immobilized $–SO_3H$ group onto the surface of a solid support is one of the most common methods to develop the novel heterogeneous acid catalysts realm [7–11]. To date, numerous solid supports have been used as anchors for sulfonic acid groups such as nano-cellulose [12], silica [13], $Fe_3O_4@SiO_2$ [14], mesoporous silica [15], γ-

Fe_2O_3@SiO_2 [16], nano-Fe_3O_4–TiO_2 [17], nano-WO_3 [18], nano–ZrO_2 [19], $CuFe_2O_4$ [20], and PEG [21]. Therefore, considering the green chemistry aspects, biopolymers have attracted much attention as supports for catalytic applications. Among them, cellulose, as one of the most important biopolymers, has received growing attention as a non-toxic, renewable, and biocompatible polymer. It has many properties, such as biocompatible, broad chemical modifying capacity, hydrophilicity, and large surface area [22–26]. Recently, it has been introduced as a versatile support in many catalysts [27–31]. Cellulose sulfuric acid as a recyclable solid acid catalyst was prepared by Shaabani's group [32] and has been applied in various organic transformations [33]. Exploring facile economical methods for separation of catalysts, magnetite nanoparticles (Fe_3O_4) has attracted much interest in recent years because they can be easily recovered from the reaction mixture using an external magnet. Concerning their specific features, such as low-toxicity, high degree of chemical stability, they have found diverse application in chemical, biomedical, and material science [34–40]. In addition, they are adaptable to large-scale production. Considering all of these advantages and in continuation of our efforts to develop environmental benign synthetic methodology [14, 20, 41–48], we report the preparation and characterization of Fe_3O_4@Cellulose sulfuric acid as a superior heterogeneous acid catalyst (Scheme 1) in the synthesis of structurally diverse functionalized pyrimido[4,5-b]quinolines and indeno fused pyrido[2,3-d]pyrimidines via one-pot condensation of 6-amino-1,3-dimethyl uracil, 1,3-dicarbonyl compounds with aromatic aldehydes in water at 80 °C.

Experimental

All chemicals were purchased from Sigma-Aldrich and Merck company and used without further purification. The progress of the reaction was monitored by TLC on commercial aluminum-backed plates of silica gel 60 F254, visualized using

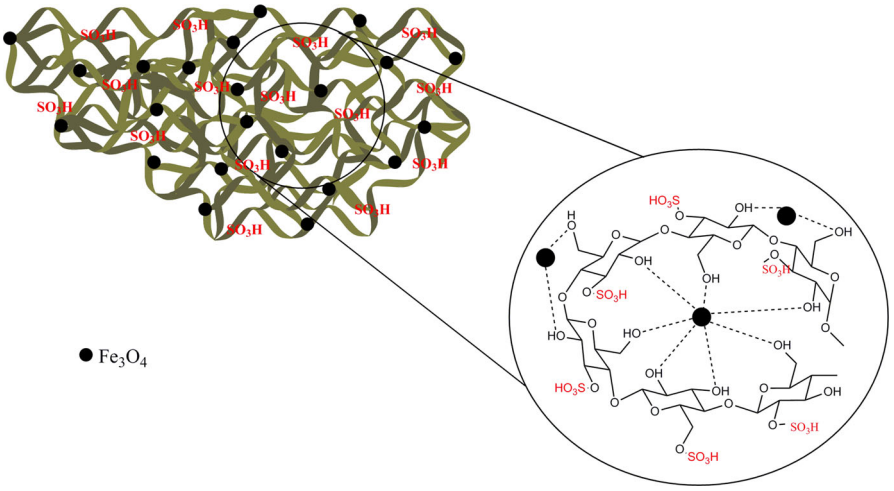

Scheme 1 Schematic representation of Fe_3O_4@Cellulose-SO_3H

ultraviolet light. Melting points were determined in open capillaries using an Electrothermal 9100 without further corrections. ^{1}H NMR and ^{13}C NMR spectra were recorded using a Bruker DRX-400 spectrometer at 400 and 100, respectively. Elemental analyses were performed on a Perkin-Elmer CHN analyzer, 2400 series II. Nano-Fe_3O_4@Celloluse-SO_3H was characterized by FT-IR spectra, which were obtained from potassium bromide pellets in the range of 400–4000 cm^{-1} using a Shimadzu 8400 s spectrometer. X-ray diffraction (XRD) was detected by Philips using Cu-Ka radiation of wavelength 1.54 Å; Scanning electron Microscopy, FE-SEM-EDX, analysis was performed using Tescanvega II XMU Digital Scanning Microscope. Samples were coated with gold at 10 mA for 2 min prior to analysis. The magnetic property of the catalyst was confirmed by using a vibrating sample magnetometer (VSM, Lakeshore7407) at room temperature. Thermogravimetric analyses (TGA) was obtained using a LINSEIS model STS PT 16,000 thermal analyzer under air atmosphere at a heating rate of 5 °C min^{-1}.

Preparation of Fe_3O_4 nanoparticles

MNPs were synthesized by co-precipitation method according to our earlier report [14].

Preparation of Fe_3O_4@Cellulose

The nano-Fe_3O_4@Cellulose composite was prepared by adding a suspension of cellulose (2 wt%) to a suspension of the MNPs in water (10 mg/mL). The obtained mixture was heated at 70 °C for 2 h. The nano-Fe_3O_4@Cellulose were isolated with external magnetic field and washed with deionized water two to three times, and then dried in an oven [49].

Preparation of Fe_3O_4@Cellulose-SO_3H

A flask equipped with a constant-pressure dropping funnel and a gas inlet tube for conducting HCl gas over an adsorbing solution was charged with Fe_3O_4@Cellulose (1 g). Then, neat chlorosulfonic acid (0.022 mL, 3 mmol) was added drop-wise over a period of 15 min in an ice bath (0–5 °C). HCl gas immediately evolved from the reaction vessel. After that, the mixture was shaken for 1 h at room temperature and Fe_3O_4@Cellulose-SO_3H was collected as a dark brown solid. The catalyst was washed with EtOH three times and dried at room temperature [13].

Loading of H^+

The optimum concentration of H^+ of Fe_3O_4@Cellulose-SO_3H was determined by acid–base potentiometric titration of the aqueous suspension of catalyst with standard NaOH solution [19]. At first, 0.1 g catalyst was dispersed in 20 mL H_2O by ultrasonic bath for 60 min at room temperature. The amount of the acid was neutralized by addition of standard NaOH solution (0.093 N) to the equivalence

point of titration. The required volume of NaOH to this point was 4.3 mL. This is equal to a loading of 3.9 mmol H^+/g.

General procedure for the synthesis of pyrimido[4,5-b]quinolones and pyrido[2,3-d]pyrimidines

Fe_3O_4@Cellulose-SO_3H (0.025 g, 0.097 mmol H^+) was added to a mixture of benzaldehyde (1.0 mmol), 6-amino-1,3-dimethyluracil (1.0 mmol), and 1,3-diketone (1.0 mmol) in distilled water (1 mL). The reaction mixture was heated in an oil bath at 80 °C with stirring for the appropriate time upon completion of the reaction, monitored by TLC, and then the reaction mixture was allowed to cool to room temperature. The obtained solid was dissolved in hot EtOH and the catalyst was separated using an external magnet. The pure products were afforded in 80–95 % yields after recrystallization in EtOH, and characterized by mp, IR, and NMR analysis.

Spectral data of new products

*5-(4-bromophenyl)-1,3-dimethyl-5,8,9,10-tetrahydropyrimido[4,5-b]quinoline-2,4,6(1H,3H,7H)-trione (**5b**)*

mp > 300 °C; IR (KBr): (ν_{max}/cm^{-1}): 3365, 1703, 1595; ^{1}H NMR(400 MHz, DMSO-d_6): δ 1.94 (m, 2H), 2.24 (m, 2H), 2.51 (m, 2H), 3.1 (s, 1H), 3.4 (s, 3H), 3.45 (s, 3H), 7–7.4 (m, 4H), 9.1 (s, 1H); ^{13}C NMR (100 MHz, DMSO-d_6): δ 21.15, 26.94, 28.11, 30.73, 33.96, 37.06, 90.10, 112.78, 119.38, 130.45, 131.04, 144.27, 146.37, 150.98, 152.22, 161.20, 195.31 ppm. Anal. Calced for $C_{17}H_{18}BrN_3O_3$: C 52.05, H 4.59, N 10.71; found: C 51.92, H 4.45, N 10.57.

*5-(4-methoxyphenyl)-1,3-dimethyl-5,8,9,10-tetrahydropyrimido[4,5-b]quinoline-2,4,6(1H,3H,7H)-trione (**5c**)*

mp 294–297 °C; IR (KBr, cm^{-1}): 3346, 2956, 1701, 1664; ^{1}H NMR(400 MHz, DMSO-d_6): δ 1.95 (m, 2H), 2.24 (m,2H), 2.55 (m,2H), 3.1 (s,1H), 3.46 (s,1H), 3.49 (s,1H), 3.67 (s,3H),6.7–7.1 (m,4H), 9.07 (S,1H); ^{13}C NMR (100 MHz, DMSO-d_6): δ 21.20, 26.93, 28.09, 30.63, 33.13, 37.14, 55.34, 90.89, 113.52, 113.58, 129.01, 139.34, 143.99, 151.00, 151.73, 157.92, 161.26, 195.39 ppm. Anal. Calced for $C_{18}H_{21}N_3O_4$: C 62.97, H 6.12, N 12.24; found: C 62.85, H 5.96, N 12.09.

Result and discussion

The route leading to nano-Fe_3O_4@Cellulose-SO_3H is illustrated in Scheme 2.

The magnetized catalyst was prepared from low cost commercially available materials. Initially, the nano-Fe_3O_4 magnetic particles have been prepared by a chemical co-precipitation in basic solution [14]. Then, the nano-Fe_3O_4@Cellulose composite was prepared simply by dispersing of the nano-Fe_3O_4 particles in

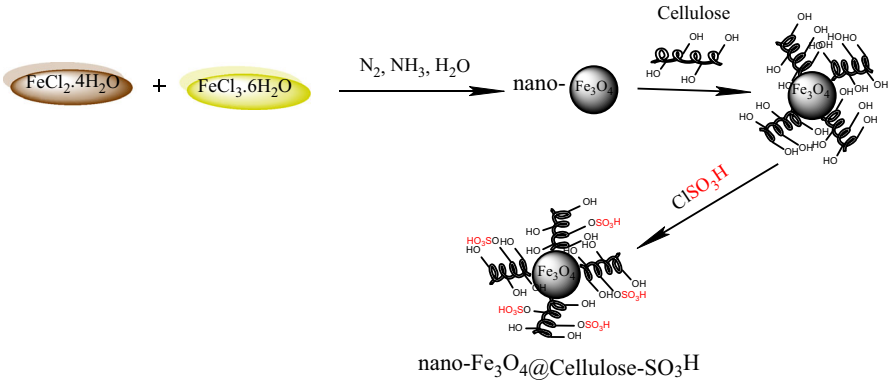

Scheme 2 Preparation of nano-Fe_3O_4@Cellulose-SO_3H

aqueous cellulose solution. The resulting magnetic composite was functionalized using chlorosulfonic acid and fully characterized by FT-IR, FE-SEM, EDX, XRD, TGA, and VSM techniques. The FT-IR spectrum of the synthesized nano-Fe_3O_4@Cellulose-SO_3H in comparison to that of nano-Fe_3O_4 and nano-Fe_3O_4@-Cellulose is shown in Fig. 1. The presence of major bands around 550 cm^{-1} is attributed to the vibration of Fe–O [50]. Typical wave numbers of the hydroxyl groups of cellulose, such as –CH–OH and –CH_2–OH stretching are in the range of 3400–3300 cm^{-1}. The methylene groups stretching, from the incorporated molecule, are located at 2900 cm^{-1} and the band in the 3000–2800 cm^{-1} range is attributed to the –C–H groups. The OH bending vibration of the cellulose surface is located at 1639 cm^{-1}, the primary and secondary hydroxyl bending appeared in

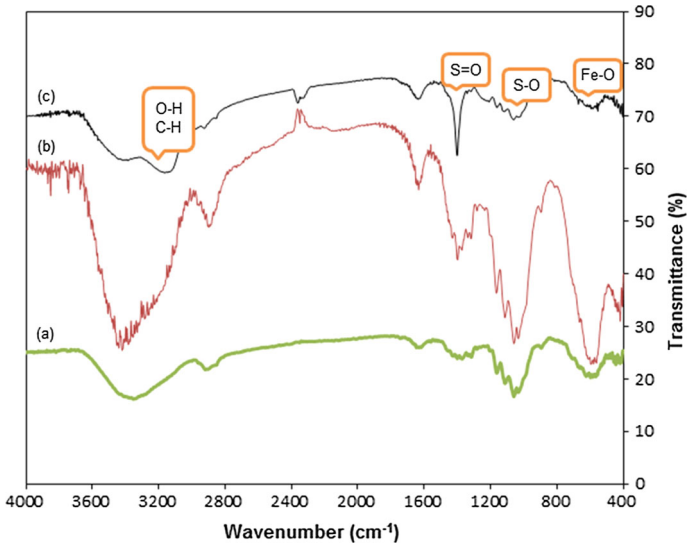

Fig. 1 FTIR spectra of Fe_3O_4 (*a*), Fe_3O_4@Cellulose (*b*), and Fe_3O_4@Cellulose-SO_3H (*c*)

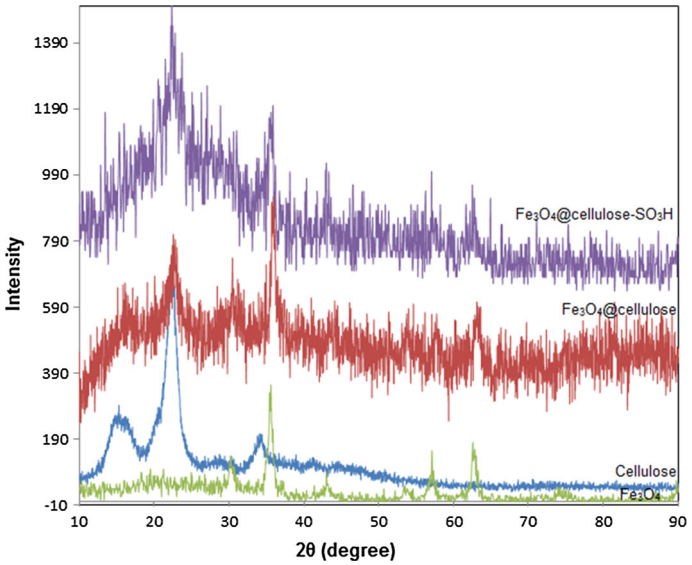

Fig. 2 The XRD pattern of Fe_3O_4, @Cellulose, Fe_3O_4@Cellulose and Fe_3O_4@Cellulose-SO_3H

the range of 1500–1200 cm^{-1}, and C–O stretching vibration is observed at 1100 cm^{-1} [51, 52].

After functionalization of nano-Fe_3O_4@cellulose composite with SO_3H group, The characteristic peaks of the OSO_3H group of chlorosulfonic acid were observed at 3300, 1581, 1288, and 1064 cm^{-1}, that corresponds to O–H, S=O, and S–O groups, respectively, indicating the presence of –OSO_3H group bonded to magnetic composite [53].

The presence of magnetite crystal phase in cellulose sulfuric acid was identified with the X-ray diffraction powder (Fig. 2). The characteristic XRD peaks of Fe_3O_4 appeared at $2\theta = 31.1°$, 39°, 45.2°, 50.43°, 56.6°, and 65.84° corresponding to the (220), (311), (400), (422), (511), and (440) planes of Fe_3O_4 crystal, that match well with standard spectra [54]. According to Debye–Scherrer formula, the average crystal size of magnetite particles was calculated to be 8.91 nm. As can be seen in the XRD pattern of Fe_3O_4@Cellulose, the position and the relative intensities of observed peaks are similar to those of nano-Fe_3O_4 and cellulose. This result confirms the presence of the Fe_3O_4 crystalline structure in the final product. Notably, the same peaks are also observed in Fe_3O_4@cellulose-SO_3H XRD spectra, which indicate the structural ability of Fe_3O_4@cellulose with –SO_3H modification [51].

The morphology and structure of synthesized composites were determined with scanning electron microscopy (SEM) (Fig. 3). The SEM image of Fe_3O_4@Cellulose composite showed that the Fe_3O_4 nanoparticles have been dispersed in a cellulose matrix (Fig. 3a). In addition the SEM image of Fe_3O_4@Cellulose-SO_3H has definitely been altered upon functionalization as shown in Fig. 3b.

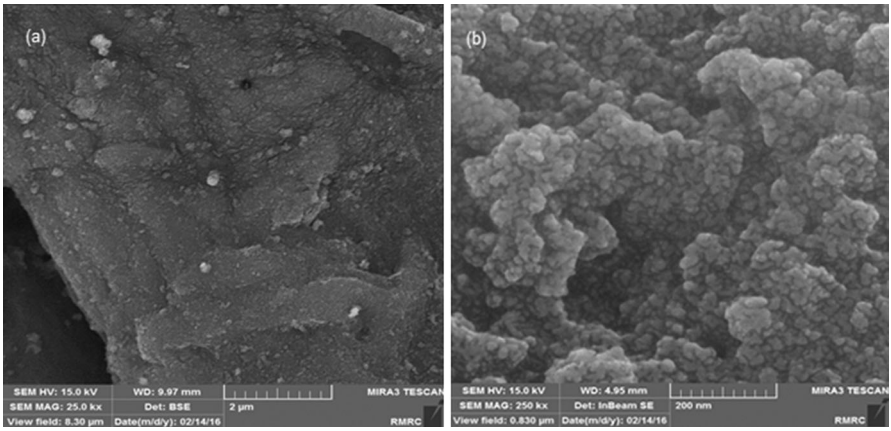

Fig. 3 FE-SEM analysis of Fe_3O_4@Cellulose (**a**), Fe_3O_4@Cellulose-SO_3H (**b**)

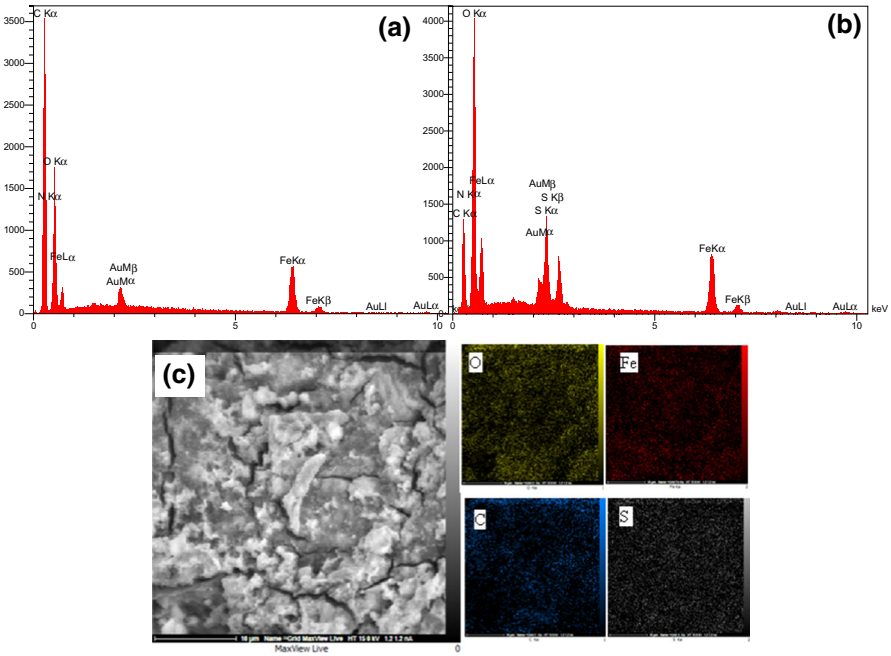

Fig. 4 EDX analysis of Fe_3O_4@Cellulose (**a**) and Fe_3O_4@Cellulose-SO_3H (**b**) and elemental mapping data of Fe_3O_4@Cellulose-SO_3H (**c**)

The EDX spectrum of Fe_3O_4@Cellulose and Fe_3O_4@Cellulose-SO_3H as an exact elemental analysis is depicted in Fig. 4 and shows the presence of C, O, and Fe of Fe_3O_4@Cellulose composite (Fig. 4a) and C, O, Fe, and S of Fe_3O_4@Cellulose-SO_3H acid catalyst, that clearly indicate the efficient preparation of Fe_3O_4@Cellulose composite. The appearance of Au elements in EDX analysis is the result of

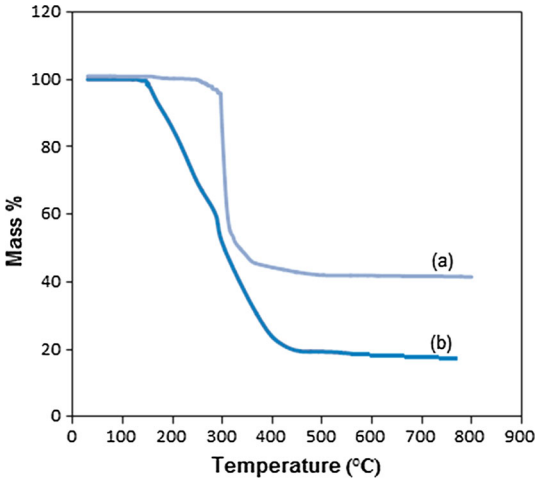

Fig. 5 TGA spectra of Fe_3O_4@Cellulose (*a*), Fe_3O_4@Cellulose-SO_3H (*b*)

the coating of materials by the layer of Au element. In addition, an elemental map of the catalyst showed the presence of S, O, C, and Fe, too.

To determine the thermal stability of the catalyst, thermogravimetric analysis (TGA) was used. TG curves of Fe_3O_4@Cellulose and Fe_3O_4@Cellulose-SO_3H are shown in Fig. 5. The weight loss of Fe_3O_4@Cellulose is about 60 % at 315–400 °C, corresponding to the thermal decomposition of cellulose chains. The pattern of mass loss was changed in TGA analysis of Fe_3O_4@Cellulose-SO_3H (Fig. 5b), which confirms the functionalization of magnetic cellulose with $–SO_3H$ [17]. Moreover, the catalyst was stable up to 200 °C, indicating its safe use at temperature range 80–150 °C in related organic reactions.

One of the most important advantages of the magnetic catalysts is their super-paramagnetic behavior, making their separation feasible by an external magnet. For this reason the magnetic property of as-synthesized acid catalyst was evaluated by VSM analysis (Fig. 6). In VSM analysis, good magnetization saturation (21.2 emu g^{-1}) and no hysteresis were ascribed to super-paramagnetic behavior of the Fe_3O_4@Cellulose-SO_3H. So it can be simply recovered using an external magnet.

To check if it is able to catalyze the reactions under study, we have considered the one-pot, three-component synthesis of functionalized pyrimido[4,5-b]quinolines and indeno fused pyrido[2,3-d]pyrimidines derivatives. In order to optimize the reaction condition, the reaction of benzaldehyde (1 mmol), uracil (1 mmol), and dimedone (1 mmol) for the synthesis of corresponding product 1,3,8,8-tetra methyl-5-phenyl-5,8.9,10-tetrahydropyrimido[4,5-b]quinolone-2,4,6(1H,3H,7H)-trione (**4a**) was selected as the model reaction (Scheme 3). In this regard, various reaction parameters such as solvent, temperature and the amount of catalyst were investigated. In addition, with particular reference to the importance of green chemistry, the model reaction was tried in water and solvent-free state as green conditions (Table 1). As Table 1 shows, in the absence of the catalyst, a low yield of the products were obtained (Table 1, entry 1).

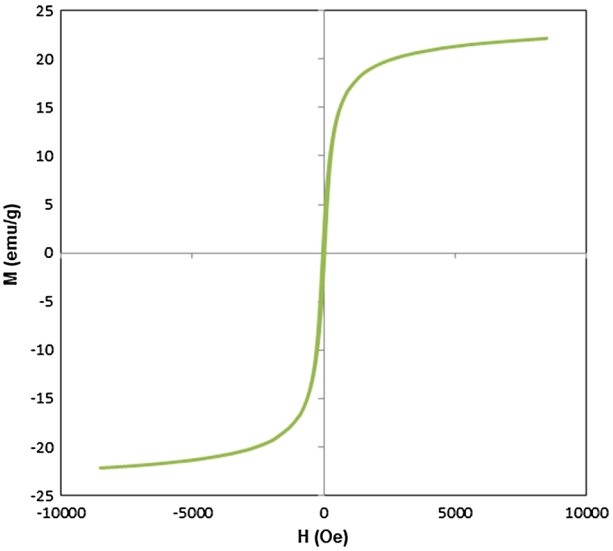

Fig. 6 VSM analysis of Fe_3O_4@Cellulose-SO_3H

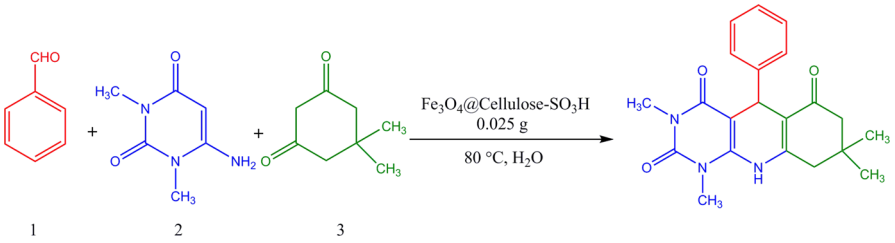

Scheme 3 The model reaction

To clarify the dependency of the catalytic activity to the presence of $–SO_3H$ group, the model reaction was conducted with Fe_3O_4 and Fe_3O_4@Cellulose. As the desired product is formed slightly in these cases, it seems to be reasonable to conclude that the catalytic effect is risen from the $–SO_3H$ group (Table 1, entries 12 and 13). Finally, the best results are obtained with the following reaction condition, 0.025 g catalyst (0.097 mmol/g H^+) at 80 °C in water (Table 1, entry 3). The keto-enol tatumerization equilibrium of the 1,3-dicarbonyl compound has been recognized as an important factor for the success of this reaction and water is a very favorable option for a solvent if a cyclic dicarbonyl reactant is employed [55, 56].

To establish the efficiency of the novel acid catalyst in previously mentioned kinds or reactions, we dealt with the reaction of the substituted aryl aldehydes and the other diketones such as 1,3-cyclohexandione and indanedione in optimized reaction condition (Scheme 4), and the results depicted in Table 2. All the

Table 1 Optimization of the three-component reaction of benzaldehyde (1), 6-amino-1,3-dimethyluracil (2), and dimedone (3) under various conditions

Entry	Catalyst	Catalyst (g)	Solvent	Temp (°C)	Time (min)	Yield[a] (%)
1	–	–	H_2O	80	360	Trace
2	Fe_3O_4@Cellulose-SO_3H	0.01	H_2O	80	60	62
3	Fe_3O_4@Cellulose-SO_3H	0.025	H_2O	80	30	95
4	Fe_3O_4@Cellulose-SO_3H	0.05	H_2O	80	30	90
5	Fe_3O_4@Cellulose-SO_3H	0.025	Free	100	65	16
6	Fe_3O_4@Cellulose-SO_3H	0.025	Ethanol	Reflux	55	50
7	Fe_3O_4@Cellulose-SO_3H	0.025	Acetonitrile	Reflux	50	45
8	Fe_3O_4@Cellulose-SO_3H	0.025	Etheylacetate	Reflux	50	50
9	Fe_3O_4@Cellulose-SO_3H	0.025	H_2O	25	180	50
10	Fe_3O_4@Cellulose-SO_3H	0.025	H_2O	70	60	67
11	Fe_3O_4@Cellulose-SO_3H	0.025	H_2O	100	85	90
12	Fe_3O_4@Cellulose	0.025	H_2O	80	30	Trace
13	Fe_3O_4	0.025	H_2O	80	30	Trace

Reaction conditions: Benzaldehyde (1.0 mmol), 6-amino-1,3-dimethyluracil (1.0 mmol), dimedone (1.0 mmol), solvent (1 mL)

[a] Isolated yields

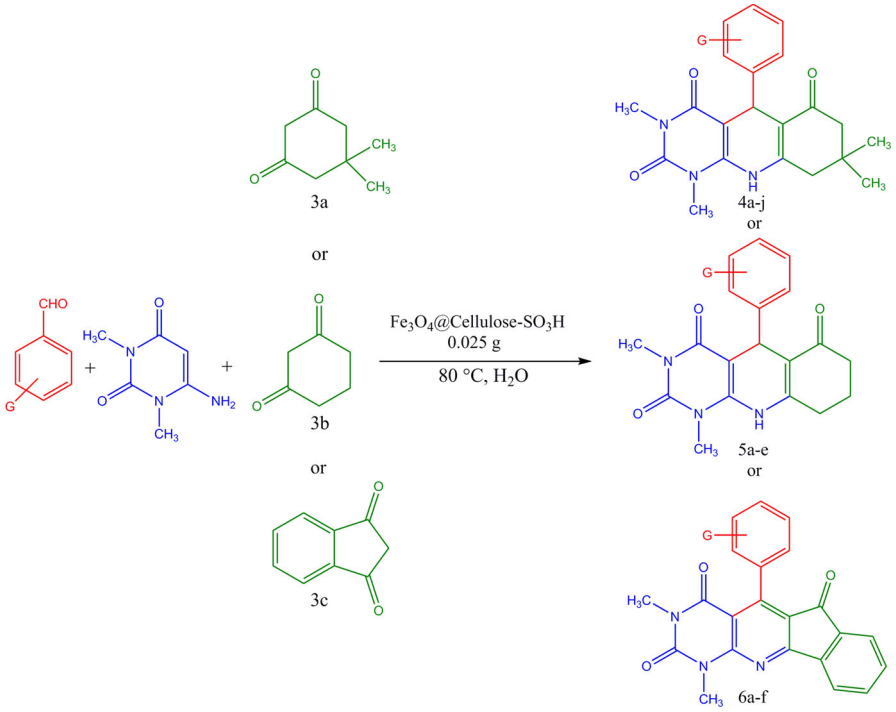

Scheme 4 Synthesis of various functionalized pyrimido[4,5-b]quinolines and indeno fused pyrido[2,3-d]pyrimidines derivatives

Table 2 Synthesis of different Pyrimido[4,5-b]quinolines (**4** and **5**) and pyrido[2,3-d]pyrimidine (**6**) in the presence of Fe_3O_4@Cellulose-SO_3H under reaction conditions

Entry	Aldehyde	Product	Diketone	Time (min)	Yield[a] (%)	Mp °C	M.P.°C [References]
1	C_6H_5CHO	**4a**	Dimedone	20	95	238	268 [57]
2	4-$MeOC_6H_4CHO$	**4b**	Dimedone	30	87	>300	>300 [57]
3	3-$O_2NC_6H_4$ CHO	**4c**	Dimedone	20	90	226–228	220–223 [57]
4	4-$O_2NC_6H_4$ CHO	**4d**	Dimedone	20	95	234	222–224 [57]
5	2-ClC_6H_4 CHO	**4e**	Dimedone	30	80	>300	>300 [57]
6	4-ClC_6H_4 CHO	**4f**	Dimedone	20	90	287	291 [57]
7	4-BrC_6H_4 CHO	**4g**	Dimedone	30	84	280	281–283 [57]
8	2-Thiophencarbaldehyde	**4h**	Dimedone	30	84	297	296–298 [57]
9	4-FC_6H_4 CHO	**4i**	Dimedone	20	80	232–236	234–236 [57]
10	2-$MeOC_6H_4CHO$	**4j**	Dimedone	40	90	>300	>300 [57]
11	4-$NO_2C_6H_4CHO$	**5a**	Cyclohexandione	30	90	300	300–302 [58]
12	4-BrC_6H_4CHO	**5b**	Cyclohexandione	90	70	>300	–
13	4-$OMeC_6H_4CHO$	**5c**	Cyclohexandione	120	84	294–297	–
14	4-ClC_6H_4CHO	**5d**	Cyclohexandione	45	85	310	>300 [58]
15	4-$(CH_3)_2NC_6H_4$	**5e**	Cyclohexandione	120	86	265–268	278–280 [58]
16	C_6H_5CHO	**6a**	Indanedione	35	85	>300	>300 [57]
17	4-MeC_6H_4CHO	**6b**	Indanedione	35	90	>300	>300 [59]
18	4-$O_2NC_6H_4CHO$	**6c**	Indanedione	30	95	258–260	254–256 [59]
19	3-$O_2NC_6H_4CHO$	**6d**	Indanedione	30	90	>300	>300 [59]
20	4-ClC_6H_4CHO	**6e**	Indanedione	30	95	>300	>300 [59]
21	4-BrC_6H_4	**6f**	Indanedione	30	95	>300	>300 [59]

Reaction condition: benzaldehyde (**1**, 1 mmol), 6-amino-1,3-dimethyluracil (**2**, 1 mmol), diketone (**3a–b–c**, 1 mmol), catalyst (0.025 g) at 80 °C in water

[a] Isolated yields

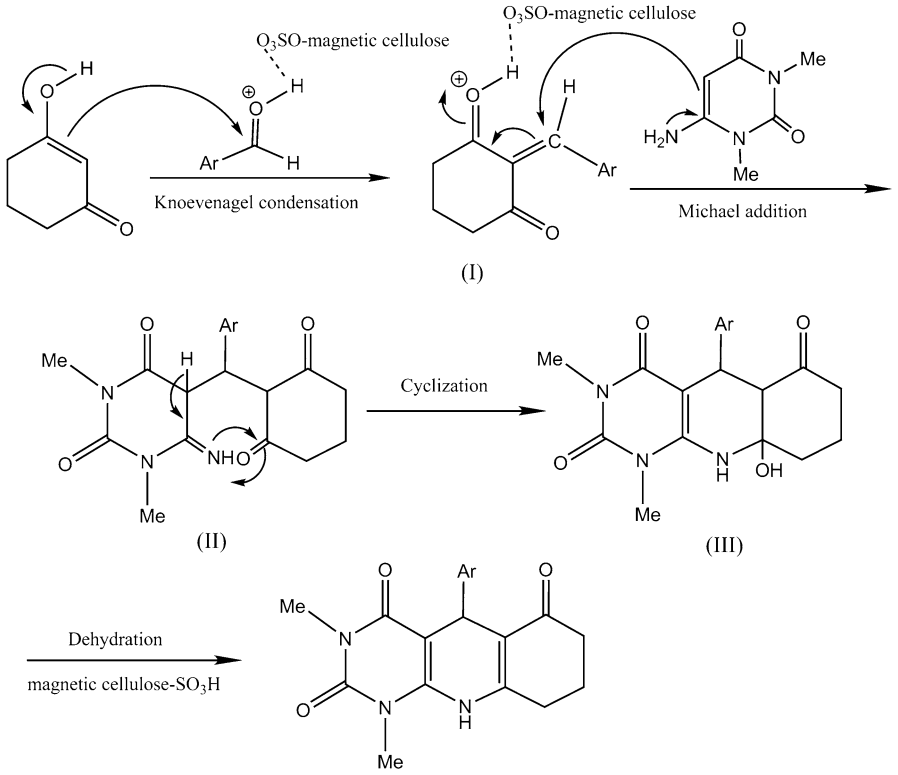

Scheme 5 The proposed mechanism

Table 3 Comparison of the efficiency of Fe_3O_4@Cellulose-SO_3H with the other reported catalysts for the synthesis of **4f**

Entry	Catalyst	Catalyst loading	Condition	Time (min)	Yield (%)
1	ρ-TSA	20 mol %	H_2O/90 °C	150	89 [60]
2	Fe_3O_4@SiO_2–SO_3H	20 mg	H_2O/70 °C	30	92 [57]
3	[bmim]Br	2 ml	H_2O/95 °C	210	90 [59]
4	Fe_3O_4@Cellulose-SO_3H	20 mg	H_2O/80 °C	20	90 (This work)

investigated arylaldehydes with either electron-donating or electron-withdrawing substituent afforded corresponding products in high yields and short reaction time.

The proposed mechanism presented sequences, including condensation, addition, cyclization, and dehydration, was reported in the literature (Scheme 5) [57, 59–61]. On the basis of the mechanism, the adduct (I) is created through the Fe_3O_4@Cellulose-SO_3H-catalyzed Knoevenagel condensation between the aldehyde and cyclic 1,3-diketone. Then, the 6-amino-1,3-dimethyluracil attacks to the adduct (I) via a Michael addition to produce an open chain intermediate (II). Subsequently, intermediate (II) undergoes intra molecular cyclization by the reaction of nucleophilic amino function to carbonyl group followed by dehydration to generate

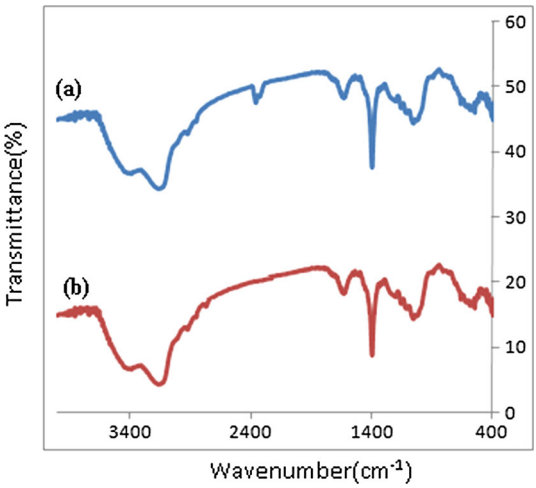

Fig. 7 FTIR of *a* fresh catalyst and *b* recycled catalyst after five runs

product (III). The aromatization take place in synthesis of indeno fused pyrido[2,3-d]pyrimidines (**6a–f**).

In order to show the advantages of the new catalyst, a comparison of the use of nano-Fe_3O_4@Cellulose-SO_3H with the other reported catalysts for the synthesis of the target products has been shown in Table 3. These results demonstrate that the new catalyst promotes the reaction more effective in terms of short reaction times and simple conditions. Furthermore, the yield of products in the presence of nano-Fe_3O_4@Cellulose-SO_3H is comparable to the reported catalysts.

The reusability and recovery of the catalyst are important issues for the catalytic reactions which make the method economically valuable, industrially profitable and environmentally sustainable. So the model reaction under optimal condition was selected to investigate the turns that the catalyst may keep holds its catalytic activity. After completion the reaction, the mixture decanted and hot ethanol added to it. The catalyst was easily separated using an external magnet, washed with ethanol, dried at 70 °C, and used for the next cycle. The recovered catalyst was added to fresh substrates of the mentioned reaction for at least five times without any noticeable reduction in catalytic activity. The yields of the five runs were found to be 95, 93, 90, 88, and 85 %, respectively. The slight decrease in the yield could probably be due to the gradual loss of the catalyst during the work-up procedure. The acidity of the understudy catalyst after five runs was measured using potentiometric titration and was obtained 3.9 mmol H^+/g that was equal to the fresh catalyst. In addition the FT-IR of this recovered sample was recorded which was identical with that of taken for the characterization of the novel prepared catalyst (Fig. 7).

Conclusion

In summary, an eco-friendly, efficient and heterogeneous acid catalyst, Fe_3O_4@-Cellulose-SO_3H was prepared, characterized and applied for one-pot, three-component synthesis of pyrimido[4,5-b]quinolones and pyrido[2,3-d]pyrimidines

derivatives. Application of cellulose as a green and recoverable biopolymer, use of water as solvent, easy recovery of catalyst, and low catalyst loading are some merits of this methodology.

Acknowledgment The authors gratefully acknowledge Semnan University Research Council for financial support of this work.

References

1. J. Safari, S. Gandomi-Ravandi, Z. Akbari, J. Adv. Res. **4**, 6 (2013)
2. I.R. Siddiqui, P. Rai, R. Rahila, H. Sagir, P. Singh, RSC Adv. **5**, 35 (2015)
3. R.M. Singh, N. Sharma, R. Kumar, M. Asthana, S. Upadhyay, Tetrahedron Lett. **68**, 50 (2012)
4. J.M. Khurana, A. Chaudhary, B. Nand, A. Lumb, Tetrahedron Lett. **53**, 24 (2012)
5. I. Devi, B.S.D. Kumar, P.J. Bhuyan, Tetrahedron Lett. **44**, 45 (2003)
6. N.A. Hassan, M.I. Hegab, F.M. Abdel-Motti, S.H.A. Hebah, F.M.E. Abdel-Megeid, A.I. Hashem, J. Heterocycl. Chem. **44**, 4 (2007)
7. A. Shaabani, Z. Hezarkhani, M.T. Faroghi, Monatsh. Chem. (2016). doi:10.1007/s00706-016-1717-7
8. M. Shamsi-Sani, F. Shirini, M. Abedini, M. Seddighi, Res. Chem. Intermed. **42**, 2 (2016)
9. E. Kolvari, N. Koukabi, M.M. Hosseini, J. Mol. Catal. A: Chem. **397**, 68 (2015)
10. A.R. Kiasat, L. Hemat-Alian, Res. Chem. Intermed. **41**, 2 (2015)
11. M. Wu, Y. Wang, D. Wang, M. Tan, P. Li, W. Wu, N. Tsubaki, J. Porous Mater. **23**, 1 (2016)
12. B. Sadeghi, M.H. Sowlat Tafti, J. Iran. Chem. Soc. **13**, 8 (2016)
13. M.A. Zolfigol, Tetrahedron **57**, 46 (2001)
14. F. Nemati, M.M. Heravi, R. Saeedi Rad, Chin. J. Catal. **33**, 11–12 (2012)
15. E. Mehrasbi, Y. Sarrafi, A. Vahid, H. Alinezhad, Res. Chem. Intermed. **41**, 7 (2015)
16. S. Mahdudi, D. Saberi, A. Heydari, J. Iran. Chem. Soc. **12**, 5 (2015)
17. A. Amoozadeh, S. Golian, S. Rahmani, RSC Adv. **5**, 57 (2015)
18. A. Amoozadeh, S. Rahmani, J. Mol. Catal. A: Chem. **396**, 96–107 (2015)
19. E. Kolvari, N. Koukabi, M.M. Hosseini, M. Vahidian, E. Ghobadi, RSC Adv. **6**, 9 (2016)
20. F. Nemati, A. Elhampour, M.B. Natanzi, S. Sabaqian, J. Iran. Chem. Soc. **13**, 6 (2016)
21. R.H. Vekariya, H.D. Patel, RSC Adv. **5**, 61 (2015)
22. A.M. Salgueiro, A.L. Daniel-da-Silva, A.V. Girão, P.C. Pinheiro, T. Trindade, Chem. Eng. J. **229**, 276–284 (2013)
23. C. Esmaeili, M. Ghasemi, L.Y. Heng, S.H.A. Hassan, M.M. Abdi, W.R.W. Daud, H. Ilbeygi, A.F. Ismail, Carbohydr. Polym. **114**, 253–259 (2014)
24. S. Rostamnia, B. Zeynizadeh, E. Doustkhah, A. Baghban, K.O. Aghbash, Catal. Commun. **68**, 77–83 (2015)
25. Y. Habibi, L.A. Lucia, O.J. Rojas, Chem. Rev. **110**, 6 (2010)
26. C. Johansson, J. Bras, I. Mondragon, P. Nechita, D. Plackett, P. Simon, D.G. Svetec, S. Virtanen, M.G. Baschetti, C. Breen, Bioresources. **7**, 2 (2012)
27. Z. Ghasemi, S. Shojaei, A. Shahrisa, RSC Adv. **6**, 61 (2016)
28. A. Shaabani, H. Nosrati, M. Seyyedhamzeh, Res. Chem. Intermed. **41**, 6 (2015)
29. L. Edjlali, R.H. Khanamiri, J. Abolhasani Monatsh. Chem. **146**, 8 (2015)
30. B. Liu, Z. Zhang, K. Huang, Cellulose **20**, 4 (2013)
31. H.R. Shaterian, F. Rigi, Res. Chem. Intermed. **40**, 5 (2014)
32. A. Shaabani, A. Rahmati, Z. Badri, Catal. Commun. **9**, 1 (2008)
33. R.H. Vekariya, H.D. Patel, ARKIVOC **1**, 136–159 (2015)
34. R.K. Sharma, S. Dutta, S. Sharma, R. Zboril, R.S. Varma, M.B. Gawande, Green Chem. **18**, 11 (2016)
35. B. Liu, Z. Zhang, ACS Catal. **6**, 326 (2016)
36. B. Liu, Y. Ren, Z. Zhang, Green Chem. **17**, 1610 (2015)
37. Z. Zhang, J. Zhen, B. Liu, K. Lv, K. Deng, Green Chem. **17**, 1308 (2015)
38. Sh Yin, J. Sun, B. Liu, Z. Zhang, J. Mater. Chem. A **3**, 4992 (2015)
39. Z. Zhang, Z. Yuan, D. Tang, Y. Ren, K. Lv, B. Liu, Chem. Sus. Chem. **7**, 3496 (2014)
40. N. Mei, B. Liu, J. Zheng, K. Lv, D. Tang, Z. Zhang, Catal. Sci. Technol. **5**, 3194 (2015)

41. F. Nemati, A. Elhampour, H. Farrokhi, M. Bagheri, Natanzi. Catal. Commun. **66**, 15 (2015)
42. F. Nemati, M.M. Heravi, A. Elhampour, RSC Adv. **5**, 57 (2015)
43. F. Nemati, S.H. Nikkhah, A. Elhampour, Chin. Chem. Lett. **26**, 11 (2015)
44. F. Nemati, A.G.G. Ghiyaei, B. Notash, M.H. Shayegan, V. Amani, Tetrahedron Lett. **55**, 25 (2014)
45. F. Nemati, A. Elhampour, S. Zulfaghari, Phosphorus, Sulfur Silicon Relat. Elem. **190**, 10 (2015)
46. F. Nemati, A. Elhampour, Res. Chem. Intermed. **42**, 7611 (2016)
47. A. Elhampour, F. Nemati, M. Kaveh, Chem. Lett. **45**, 223 (2016)
48. A. Elhampour, F. Nemati, J. Chin. Chem. Soc. **63**, 653 (2016)
49. L.C. Fidale, M. Nikolajski, T. Rudolph, S. Dutz, F.H. Schacher, T. Heinze, J. Colloid Interface Sci. **390**, 1 (2013)
50. M.H. Beyki, M. Bayat, S. Miri, F. Shemirani, H. Alijani, Ind. Eng. Chem. Res. **53**, 39 (2014)
51. X. Sun, L. Yang, Q. Li, J. Zhao, X. Li, X. Wang, H. Liu, Chem. Eng. J. **241**, 174–183 (2014)
52. P.V. Chavan, K.S. Pandit, U.V. Desai, M.A. Kulkarni, P.P. Wadgaonkar, RSC Adv. **4**, 79 (2014)
53. H.R. Shaterian, M. Ghashang, M. Feyzi, Appl. Catal. A **345**, 2 (2008)
54. S. Peng, H. Meng, Y. Ouyang, J. Chang, Ind. Eng. Chem. Res. **53**, 6 (2014)
55. H.M. Savanur, R.G. Kalkhambkar, G. Aridoss, K.K. Laali, Tetrahedron Lett. **57**, 3029 (2016)
56. J.H. Clark, D.J. Macquarrie, J. Sherwood, Chem. Eur. J. **19**, 5174 (2013)
57. F. Nemati, R. Saeedirad, Chin. Chem. Lett. **24**, 5 (2013)
58. K. Tabatabaeian, A.F. Shojaei, F. Shirini, S.Z. Hejazi, M. Rassa, Chin. Chem. Lett. **25**, 2 (2014)
59. S.-J. Ji, S.-N. Ni, F. Yang, J.-W. Shi, G.-L. Dou, X.-Y. Li, X.-S. Wang, D.-Q. Shi, J. Heterocycl. Chem. **45**, 3 (2008)
60. G.K. Verma, K. Raghuvanshi, R. Kumar, M.S. Singh, Tetrahedron Lett. **53**, 4 (2012)
61. K. Mohammadi, F. Shirini, A. Yahyazadeh, RSC Adv. **5**, 23586 (2015)